Development/Plasticity/Repair

Mechanisms of Enhanced Phrenic Long-Term Facilitation in *SOD1*^{G93A} Rats

Nicole L. Nichols,[1,2] **Irawan Satriotomo,**[1,3] **Latoya L. Allen,**[1] **Ashley M. Grebe,**[1] **and Gordon S. Mitchell**[1,3]

[1]Department of Comparative Biosciences, University of Wisconsin-Madison, Madison, Wisconsin 53706, [2]Department of Biomedical Sciences, University of Missouri, Columbia, Missouri 65211, and [3]Center for Respiratory Research and Rehabilitation, Department of Physical Therapy and McKnight Brain Institute, University of Florida, Gainesville, Florida 32611-0154

Amyotrophic lateral sclerosis (ALS) is a degenerative motor neuron disease, causing muscle paralysis and death from respiratory failure. Effective means to preserve/restore ventilation are necessary to increase the quality and duration of life in ALS patients. At disease end-stage in a rat ALS model (*SOD1*^{G93A}), acute intermittent hypoxia (AIH) restores phrenic nerve activity to normal levels via enhanced phrenic long-term facilitation (pLTF). Mechanisms enhancing pLTF in end-stage *SOD1*^{G93A} rats are not known. Moderate AIH-induced pLTF is normally elicited via cellular mechanisms that require the following: G_q-protein-coupled 5-HT_2 receptor activation, new BDNF synthesis, and MEK/ERK signaling (the Q pathway). In contrast, severe AIH elicits pLTF via a distinct mechanism that requires the following: G_s-protein-coupled adenosine 2A receptor activation, new TrkB synthesis, and PI3K/Akt signaling (the S pathway). In end-stage male *SOD1*^{G93A} rats and wild-type littermates, we investigated relative Q versus S pathway contributions to enhanced pLTF via intrathecal (C4) delivery of small interfering RNAs targeting BDNF or TrkB mRNA, and MEK/ERK (U0126) or PI3 kinase/Akt (PI828) inhibitors. In anesthetized, paralyzed and ventilated rats, moderate AIH-induced pLTF was abolished by siBDNF and UO126, but not siTrkB or PI828, demonstrating that enhanced pLTF occurs via the Q pathway. Although phrenic motor neuron numbers were decreased in end-stage *SOD1*^{G93A} rats (~30% survival; $p < 0.001$), BDNF and phosphorylated ERK expression were increased in spared phrenic motor neurons ($p < 0.05$), consistent with increased Q-pathway contributions to pLTF. Our results increase understanding of respiratory plasticity and its potential to preserve/restore breathing capacity in ALS.

Key words: breathing; disease; neurodegenerative; plasticity; spinal cord

Significance Statement

Since neuromuscular disorders, such as amyotrophic lateral sclerosis (ALS), end life via respiratory failure, the ability to harness respiratory motor plasticity to improve breathing capacity could increase the quality and duration of life. In a rat ALS model (*SOD1*^{G93A}) we previously demonstrated that spinal respiratory motor plasticity elicited by acute intermittent hypoxia is enhanced at disease end-stage, suggesting greater potential to preserve/restore breathing capacity. Here we demonstrate that enhanced intermittent hypoxia-induced phrenic motor plasticity results from amplification of normal cellular mechanisms versus addition/substitution of alternative mechanisms. Greater understanding of mechanisms underlying phrenic motor plasticity in ALS may guide development of new therapies to preserve and/or restore breathing in ALS patients.

Introduction

The nervous system regulates breathing by complex mechanisms of sensory feedback, sensory feedforward, and adaptive control (i.e., neuroplasticity; Mitchell et al., 1990, 2007, 2009). One major site of neuroplasticity in the neural system controlling breathing is within respiratory motor nuclei that drive respiratory muscles (Feldman et al., 2003; Mitchell and Johnson, 2003). When phrenic motor neurons innervating the diaphragm are compromised by

Received Nov. 30, 2016; revised April 8, 2017; accepted May 5, 2017.

Author contributions: N.L.N. and G.S.M. designed research; N.L.N., I.S., L.L.A., and A.M.G. performed research; N.L.N., I.S., L.L.A., and A.M.G. analyzed data; N.L.N. wrote the paper.

This work was supported by National Institutes of Health (NIH) Grants HL119606 (N.L.N), NS057778 (G.S.M.), HL69064 (G.S.M.), and HL080209 (G.S.M.). N.L.N. was also supported by fellowships from the NIH (T32 HL007654) and the Francis Families Foundation. L.L.A. was supported by the McNair Scholar Program. L.L.A. and A.M.G. were supported by the Integrated Biological Sciences Summer Research Program. We thank Kalen Nichols for assistance with blood-gas analysis, Safraaz Mahammed for the custom-designed computer program used for data analysis, and Patrick Mulcrone and Michael Meyer for maintenance and genotyping of the rat colony.

The authors declare no competing financial interests.

Correspondence should be addressed to Dr. Nicole Nichols, Department of Biomedical Sciences, University of Missouri., 1600 East Rollins Street, Columbia, MO 65211. E-mail: nicholsn@missouri.edu.

L. L. Allen's present address: Department of Neuroscience, University of Florida, Gainesville, FL 32611-0154.

A. M. Grebe's present address: Inpatient Physical Therapy Department, Shirley Ryan AbilityLab, Chicago, IL 60611.

DOI:10.1523/JNEUROSCI.3680-16.2017

 0270-6474/17/375834-12$15.00/0

neuromuscular injury or disease, breathing ability can be compromised, threatening life itself. Spontaneous or induced phrenic motor plasticity can slow or even improve breathing capacity when the respiratory system has been compromised (Mitchell, 2007; Gonzalez-Rothi et al., 2015).

Multiple cellular mechanisms give rise to phrenic motor plasticity, expressed as long-lasting phrenic motor facilitation (pMF; Dale-Nagle et al., 2010; Devinney et al., 2013). The specific form of pMF elicited by acute intermittent hypoxia (AIH; Baker and Mitchell, 2000; Fuller et al., 2000; Baker-Herman and Mitchell, 2002) is known as phrenic long-term facilitation (pLTF). The dominant cellular mechanism contributing to pLTF following moderate AIH is known as the Q pathway to pMF (Dale-Nagle et al., 2010) because it is initiated by G_q-protein-coupled $5HT_2$ receptors (Fuller et al., 2000). The Q pathway requires new synthesis of brain-derived neurotrophic factor (BDNF; Baker-Herman et al., 2004) and extracellular signal-regulated protein kinase (ERK) activation via mitogen extracellular kinase (MEK; Hoffman et al., 2012). In contrast, following severe AIH, the dominant mechanism of pLTF is known as the S pathway to pMF (Dale-Nagle et al., 2010; Nichols et al., 2012) because it is initiated by G_s-protein-coupled metabotropic receptors, including adenosine 2A (A_{2A}; Golder et al., 2008; Nichols et al., 2012) or $5\text{-}HT_7$ receptors (Hoffman and Mitchell, 2011). The S pathway requires new synthesis of immature tropomyosin-related kinase B (TrkB) receptor isoform (Golder et al., 2008; Hoffman and Mitchell, 2011; vs BDNF) and activation of protein kinase B (pAkt; vs ERK) via phosphatidylinositol 3-kinases (PI3K; Golder et al., 2008; Hoffman and Mitchell, 2011).

Understanding mechanisms that control and/or constrain AIH-induced pLTF informs us as we explore the role of plasticity in disease models, such as amyotrophic lateral sclerosis (ALS). ALS is a progressive neurodegenerative disease that results in phrenic motor neuron death, ultimately leading to ventilatory failure in ALS patients (Bourke et al., 2001; Lyall et al., 2001; Lechtzin et al., 2002; Iłzecka et al., 2003; Kiernan et al., 2011; Singh et al., 2011; Zinman and Cudkowicz, 2011). No effective treatment strategies are currently available that alter the course of ALS disease progression.

In an ALS animal model, *SOD1*^{G93A} (Rosen et al., 1993; Gurney et al., 1994; Howland et al., 2002), major loss of phrenic motor neurons is observed at disease end-stage (Nichols et al., 2013). Despite ~80% loss of phrenic motor neurons, phrenic nerve activity is reduced only ~50%, representing >2-fold amplification of activity in spared motor neurons (Nichols et al., 2013; Nichols and Mitchell, 2016). We wondered whether moderate AIH (mAIH) could further amplify phrenic motor output and preserve/restore breathing capacity, and were surprised to discover that pLTF is actually enhanced in end-stage *SOD1*^{G93A} rats (Nichols et al., 2013, 2015). However, the mechanisms enhancing mAIH-induced pLTF in end-stage *SOD1*^{G93A} rats remain unknown.

Here, we tested the hypothesis that combined contributions from both the Q and S pathways to pMF enhance pLTF in end-stage *SOD1*^{G93A} rats. First, we prevented new BDNF or TrkB protein synthesis by applying small interfering RNAs (siRNAs) targeting BDNF or TrkB mRNA to the C_4 spinal segment before mAIH in end-stage *SOD1*^{G93A} rats and wild-type littermates. Next, we used intrathecal inhibitors of MEK (UO126) or PI3K (PI828) to inhibit activation of ERK and Akt, respectively. Last, we analyzed BDNF and phosphorylated-ERK (pERK) protein expression in phrenic motor neurons. Contrary to our hypothesis, we found that enhanced pLTF in end-stage *SOD1*^{G93A} rats results from increased Q-pathway contributions, without evidence for additional contributions from the S pathway.

Materials and Methods

Animals. Experiments were performed using adult male Sprague Dawley rats from transgenic sires overexpressing the human *SOD1*^{G93A} gene (Taconic Laboratories) bred to female wild-type Taconic Sprague Dawley rats. Heterozygous *SOD1*^{G93A} progeny were identified with PCR of tail DNA with primers specific for hSOD1. Male rats that showed disease onset ~120–140 d were used as breeders to minimize genetic drift in the colony. Rats were maintained on a 12:12 light/dark cycle with food and water *ad libitum*. *SOD1*^{G93A} rats began to show signs of muscle weakness, weight loss, and gait changes at ~120–140 d, whereas limb paralysis began at 150–180 d. Rats were considered end stage when they had lost >20% of body weight as in previous studies from our group (Nichols et al., 2013, 2015). *SOD1*^{G93A} rats were compared with wild-type littermates. All animal procedures were approved by the Institutional Animal Care and Use Committee at the School of Veterinary Medicine, University of Wisconsin, and were in agreement with standards set forth in the National Institutes of Health (NIH) *Guide for Care and Use of Laboratory Animals*. The University of Wisconsin is accredited by Association for Assessment and Accreditation of Laboratory Animal Care and is covered by NIH Assurance (A3368-01).

Neurophysiology experiments. Rats were prepared for neurophysiological experiments as described previously (Hoffman et al., 2012; Nichols et al., 2012). Wild-type and end-stage *SOD1*^{G93A} rats were induced with isoflurane (3.5% in 50% O_2, balance N_2); isoflurane anesthesia was maintained throughout surgical procedures. Rats were trachotomized, pump-ventilated (Rodent Ventilator, model 683, Harvard Apparatus; tidal volume, 2.5 ml), and bilaterally vagotomized. A polyethylene catheter (PE50; inner diameter, 0.58 mm; outer diameter, 0.965 mm; Intramedic) was inserted into the right femoral artery to monitor blood pressure (Gould-Statham P23ID pressure transducer) and blood gases using a blood gas analyzer (ABL 800, Radiometer). A rectal thermometer (Thermo Fisher Scientific) was used to monitor body temperature, which was maintained (37.5 ± 1°C) with a heated surgical table. To monitor end-tidal PCO_2 (P_{ETCO2}), a flow-through carbon dioxide analyzer was used with sufficient response time to measure P_{ETCO2} in rats (Capnogard, Novametrix). P_{ETCO2} was maintained at ~45 mmHg throughout surgical procedures. The left phrenic nerve was isolated (dorsal approach), cut distally, desheathed, and covered with a saline-soaked cotton ball until protocols commenced. Laminectomy was performed at cervical level 2 (C2) for all rats for intrathecal delivery of drugs. Once surgery was complete, rats were slowly converted to urethane anesthesia over 20–30 min (1.8 g kg^{-1}, i.v.). The adequacy of anesthesia was tested before protocols commenced and immediately after the protocol was complete; adequacy of anesthetic depth was assessed as the lack of pressor or respiratory neural response to a toe pinch with a hemostat (Bach and Mitchell, 1996; Hoffman et al., 2012; Nichols et al., 2012). Once rats were converted to urethane anesthesia, a minimum of 1 h was allowed before the experimental protocol commenced. After conversion to urethane anesthesia, rats were given a continuous intravenous infusion (1.5–6 ml kg^{-1} h^{-1}) of a 1:2:0.13 mixture of 6% hetastarch in 0.9% sodium chloride, lactated Ringer's solution, and 8.4% sodium bicarbonate to maintain appropriate blood volume, fluid, and acid–base balance.

Phrenic nerve activity was recorded with bipolar silver electrodes, amplified (10,000×), bandpass-filtered (300–10,000 Hz; model 1800, A-M Systems), rectified, and integrated (Paynter filter; time constant, 50 ms; MA-821, CWE). Integrated nerve bursts were digitized (8 kHz) and analyzed using the WINDAQ data-acquisition system (DATAQ Instruments). A small incision was made in the dura and a soft silicone catheter (2 Fr; Access Technologies) was inserted caudally 3–4 mm until the tip rested over the C4 segment to deliver drugs or siRNAs near the phrenic motor nucleus before mAIH [three 5 min episodes of isocapnic hypoxia; partial pressure of arterial O_2 (PaO_2), 35–45 mmHg] separated by 5 min intervals of baseline oxygen levels (PaO_2, ≥150 mmHg). The catheter was attached to a 50 μl Hamilton syringe filled with drug or vehicle solutions as described below. Rats were paralyzed using pancuronium

bromide to prevent spontaneous breathing efforts (2.5 mg kg^{-1}, i.v.; Bach and Mitchell, 1996).

To determine contributions of specific protein synthesis to pLTF in *SOD1*^{G93A} rats, siRNAs were delivered intrathecally (two 10 μl injections separated by 10 min) targeting either BFNF (siBDNF; ON-TARGETplus, Dharmacon; gene, *Rat BDNF*; GenBank accession number, NM 012513) or TrkB (siTrkB; ON-TARGETplus; Dharmacon; gene, *Rat NTRK2*; GenBank accession number, NM 012731) mRNA to prevent the translation and new BDNF or TrkB protein synthesis. We used a nontargeting siRNA sequence (siNT; ON-TARGETplus Nontargeting siRNA #1; Dharmacon) as a negative control for potential nonspecific effects of siRNAs. These injections took place ~2 h before the start of the AIH protocol in end-stage *SOD1*^{G93A} and wild-type rats. siRNAs were prepared as described previously (Baker-Herman et al., 2004; Golder et al., 2008; Hoffman and Mitchell, 2011; Hoffman et al., 2012). Briefly, a pool of siRNAs targeting TrkB or BDNF mRNA was reconstituted with siRNA Universal Buffer (Dharmacon) and stored at −20°C. Stock siTrkB or siBDNF (4 μl of 5 μM solution) were combined with siNT (4 μl of 5 μM solution) so that the same amount of total siRNA was used for all groups, the transfection reagent oligofectamine (32 μl; Invitrogen), and RNAase-free water (160 μl; final concentration, 100 nM), and then incubated at room temperature for 20 min. siNT experiments were performed by taking the stock siNT solution (8 μl of 5 μM solution), oligofectamine (32 μl), and RNase-free water (160 μl; final concentration, 100 nM) and then incubated as described above. Wild-type groups included three that received AIH treatment—siBDNF ($n = 8$), siTrkB ($n = 9$), and siNT ($n = 8$)—and one that received no AIH treatment—time controls (TCs; 32 μl oligofectamine + 168 μl of RNase-free water; $n = 8$). *SOD1*^{G93A} groups included three that received AIH treatment—siBDNF ($n = 5$), siTrkB ($n = 5$), siNT ($n = 5$)—and one that received no AIH treatment—TC ($n = 4$). Approximately 2 h after siRNA delivery, animals were exposed to either AIH or no AIH (TC) and phrenic nerve activity was recorded for 60 min after AIH or sham AIH.

In separate experiments, the following inhibitors were delivered intrathecally to determine the contributions of ERK MAPK or Akt to mAIH-induced pLTF in *SOD1*^{G93A} rats: (1) UO126 [1,4-diamino-2,3-dicyano-1,4-bis(*o*-aminophenylmercapto)butadiene; 12 μl, 100 μM; MEK/ERK inhibitor; Promega]; and (2) PI828 [2-(4-Morpholinyl)-8-(4-aminopheny)l–4*H*-1-benzopyran-4-one; 12 μl, 100 μM; PI3K/Akt inhibitor; Tocris Bioscience]. Wild-type treatment groups included the following: UO126 + AIH ($n = 8$), UO126 TC (no AIH; $n = 5$), PI828 + AIH ($n = 8$), PI828 TC ($n = 5$), and vehicle + AIH (12 μl, 20% DMSO; $n = 8$). *SOD1*^{G93A} treatment groups included the following: UO126 + AIH ($n = 8$), UO126 TC ($n = 5$), PI828 + AIH ($n = 8$), PI828 TC ($n = 5$), and vehicle + AIH ($n = 8$). All TC treated rats were grouped together within wild-type and *SOD1*^{G93A} rats.

To begin a protocol, the apneic threshold was determined by lowering P_{ETCO2} until nerve activity ceased for ~1 min. The recruitment threshold was then determined by slowly increasing the P_{ETCO2} until nerve activity resumed (Bach and Mitchell, 1996). P_{ETCO2} was raised to ~2 mmHg above the recruitment threshold and ~15–20 min were allowed to establish stable neural activity (i.e., baseline). An arterial blood sample was drawn after a stable baseline was achieved and throughout the protocol. Blood samples were analyzed for partial pressures of PaO_2 and $PaCO_2$ from samples drawn during baseline, the first hypoxic episode, and at 15, 30, and 60 min after AIH. Criteria for blood gases were as follows: PaO_2, ≥150 mmHg before and after AIH; $PaCO_2$ was maintained ±1.5 mmHg of baseline levels by adjusting inspired CO_2 or ventilator rate. Rats then received AIH or continuous exposure to baseline oxygen levels (sham AIH). Following the third hypoxic episode, rats were returned to baseline O_2 levels, which were maintained throughout the protocol.

Immunohistochemistry. Rats were processed to assess phrenic motor neuron survival and BDNF or phosphorylated (activated) ERK expression. Rats were either taken immediately upon the conclusion of neurophysiological protocols (for phrenic motor neuron counts) or killed with Beuthanasia (0.1 μl/g, i.p.; Intervet Schering-Plough Animal Health; for BDNF or pERK expression) without being subjected to neurophysiology experiments for protein immunohistochemistry. The rats were perfused transcardially with ice-cold 0.1 M PBS, pH~7.4, followed by ice-cold 4% paraformaldehyde in PBS, pH~7.4. After fixation, spinal cord tissues were harvested, post-fixed overnight, and cryoprotected in 30% sucrose at 4°C until sinking. Transverse sections containing phrenic motor neurons (C4; 40 μm) were cut using a freezing microtome (SM 2000R, Leica) and stored at −20°C in antifreeze solution until processed.

Cervical (C4) spinal cord sections (six per animal) taken from wild-type and *SOD1*^{G93A} rats were stained using NeuN immunohistochemistry for putative phrenic motor neuron counts. Sections were first separated and washed with 1× PBS (diluted from 10× PBS Liquid Concentrate, OmniPur, Calbiochem) three times for a period of 5 min per wash, with each animal's tissue contained in separate wells. To prevent nonspecific binding of antibody, blocker consisting of 5% normal goat serum (NGS), 1× PBS, and 0.2% Triton was added to each tissue sample, and incubated for 1 h at room temperature. Primary antibody solution was added, consisting of 5% NGS, 1× PBS, 0.1% Triton, and the antibody against neuronal nuclei (NeuN; Millipore, catalog #MAB377, RRID:AB_2298772; 1:500). Sections were incubated overnight in the primary antibody solution on a shaker at 4°C. The following day, tissues were washed three times with 1× PBS (5 min each), and then incubated in the secondary antibody solution in the dark on a shaker for 2 h at room temperature. The secondary antibody solution consisted of 5% NGS, 1× PBS, 0.1% Triton, and the secondary antibody goat anti-mouse green fluorescent Alexa 488 (1:500; Invitrogen). Following incubation, tissues were washed with 1× PBS using the same procedure (3×, 5 min each). Finally, sections were mounted on positively charged glass slides, covered with anti-fade (Prolong Gold anti-fade reagent, Molecular Probe, Life Technologies; to prevent quenching of fluorescence), coverslipped, and air-dried. Sections incubated without primary or secondary antibodies served as negative controls. Slides were stored at −20°C until quantification of staining was performed by a blinded investigator.

Cervical (C4) spinal cord sections (six per animal) taken from wild-type and *SOD1*^{G93A} rats ($n = 6$ each) were stained using immunohistochemistry techniques to compare the expression of BDNF or pERK. Free-floating sections were washed in 0.1 M PBS with 0.1% Triton X-100 (PBS-Tx; 3×, 5 min each) and incubated (30 min) in PBS containing 1% H_2O_2. After washing (3×, 5 min each) in PBS-Tx, tissues were blocked (60 min) with 5% NGS. Sections were incubated with either polyclonal rabbit anti-BDNF (N-20; 1:1000; Santa Cruz Biotechnology) or monoclonal rabbit anti-pERK [phospho-p44/42 mitogen activated protein (Erk1/2); Cell Signaling Technology, catalog #4376S RRID:AB_331772] overnight at 4°C. The next day, tissue was washed in PBS-Tx (3×, 5 min each) and incubated with secondary antibodies in biotinylated anti-rabbit (Vector Laboratories) for 60 min at room temperature. Conjugation with avidin–biotin complex (Vectastain Elite ABC kit, Vector Laboratories) was followed by visualization with 3,3′-diaminobenzidine tetrahydrochloride-hydrogen-peroxide (DAB Substrate Kit, Vector Laboratories) according to the manufacturer's instructions. Nissl-counterstained sections (0.1% cresyl-violet for 15 min, and rinsed in distilled water) enabled visualization of putative phrenic motor neurons and colocalization with pERK label. Stained sections were mounted on gelatin-coated glass slides, air-dried, dehydrated through graded alcohol (70–100%), cleared in xylene, and coverslipped using Eukitt (Electron Microscope Science). Sections incubated without primary or secondary antibodies served as negative controls. In addition, we preadsorbed the primary BDNF antibody with a fivefold (by concentration) excess of specific blocking peptides (sc-546, Santa Cruz Biotechnology). Slides were stored at −20°C until quantification of staining was performed by a blinded investigator.

Phrenic motor neuron counts. C1-ES program software and live confocal microscopy (Nikon Eclipse TE2000-U) were used to take photomicrographs (both 10× and 20×) of phrenic motor neurons in C4 spinal cord tissues. Phrenic motor neurons in the C4 ventral horn were identified and manually counted based on diagrams from *The Spinal Cord* by Watson et al. (2009), and extensive experience using retrograde labeling of phrenic motor neurons with cholera-toxin B fragment in normal rats (Dale-Nagle et al., 2011; Dale et al., 2012). Putative phrenic motor neurons were counted as described previously (Nichols et al., 2013, 2015), where the area containing phrenic motor neurons was identified as a discrete cluster of large neurons in the mediolateral C4 ventral horn

(Boulenguez et al., 2007; Mantilla et al., 2009; Watson et al., 2009). Healthy phrenic motor neurons were characterized as those exhibiting a NeuN-positive stain and an identifiable cell body and nucleus. NeuN (+) putative phrenic motor neurons were blindly counted on both left and right sides of C4 spinal cord sections for each treatment group, entered into Microsoft Excel, and averaged across sections in each rat to enable statistical comparisons between $SOD1^{G93A}$ rats and wild-type littermates. Phrenic motor neuron counts in the C4 segment were extrapolated from every sixth section (length of C4 phrenic motor nucleus, ~2000 μm; 40 μm sections) as described previously (Nichols et al., 2013, 2015).

Quantification and analysis of BDNF and pERK. Sections were numbered sequentially, and every sixth section was selected for immunohistochemistry, enabling systematic sampling. Six sections at the C4 segmental level from each rat in each group were used for immunohistochemical quantification performed by a blinded investigator. Digital photomicrographs of immunoreactive labeling in the phrenic motor nucleus were taken with the 20× objective lens (Qcapture Pro 6.0, QImaging), including appropriate controls. Densitometry for BDNF and pERK staining was performed using ImageJ software (National Institutes of Health; http://rsb.info.nih.gov/ij; RRID: SCR_003070). Images were converted to eight-bit resolution, and the threshold was set between 120 and 160 during all analyses as performed previously (Dale-Nagle et al., 2011; Dale et al., 2012; Lovett-Barr et al., 2012). A threshold was chosen for all groups for both BDNF and pERK in which all motor neurons were visible, but not saturated; images from both wild-type and $SOD1^{G93A}$ rats were treated identically in each group, and the "limit to threshold" option was selected in ImageJ to prevent the program from autothresholding. Optical density (OD) was measured within circumscribed putative phrenic motor neuron somata (location determined as described above) for BDNF and pERK immunostaining, and expressed as an average OD per unit area per individual cell. OD was measured in all putative phrenic motor neurons per section per animal, and then combined for analyses across groups. OD was averaged across motor neurons within each section, across sections within each rat, and then across rats within each group; no significant differences among rats within a group were detected (data not shown), indicating that estimates were consistent from animal to animal. For each putative phrenic motor neuron, BDNF and pERK immunofluorescence OD was expressed as a fraction of the average OD in putative phrenic motor neurons of wild-type littermates. Thus, mean OD in wild-type littermates is 1.0, with a variance reflecting rat variation within that group; differences from 1.0 demonstrate changes in $SOD1^{G93A}$ rats relative to their littermate controls. This normalized OD served as a measure of relative protein concentration of BDNF and pERK in immunopositive cells, and reflected variance among rats within that experimental group (SE).

Analysis. Integrated phrenic nerve burst amplitudes and frequency were averaged over 1 min during baseline and 15, 30, and 60 min after AIH. Phrenic nerve burst amplitude is the voltage of the integrated signal, expressed as a percentage change from baseline. Nerve burst frequency was expressed as an absolute change from baseline (bursts/min). Statistical comparisons between treatment groups for AIH studies [amplitude, frequency, $PaCO_2$, PaO_2, and mean arterial pressure] were done using a two-way ANOVA with a repeated-measures design. Since no differences were detected between successive hypoxic exposures within groups (data not shown), comparisons of the short-term hypoxic phrenic response were made using one-way ANOVA of phrenic burst amplitude during the fifth minute of hypoxic episodes averaged from all three episodes. For TC rats (no AIH), a two-way ANOVA with repeated-measures design was performed; since there were no differences among them, they were grouped into a single TC group in subsequent analyses. Although there were no significant differences in $SOD1^{G93A}$ rats treated as TCs, there was a statistically significant difference at 15 min after hypoxia for wild-type rats treated as TCs when comparing UO126 with PI828 and oligofectamine + water (phrenic activity was smaller in UO126-treated rats). Despite this lone difference, we felt justified in grouping TCs together since the apparent UO126 effect was small, and previous studies never reported similar effects in UO126-treated TC experiments (Dale-Nagle et al., 2011; Dale et al., 2012; Hoffman et al., 2012).

For immunohistochemical analyses (phrenic motor neuron counts and BDNF and pERK OD), data were compared between $SOD1^{G93A}$ and wild-type treatment groups using a one-way ANOVA. Since no significant differences existed for phrenic motor neuron survival within $SOD1^{G93A}$ or wild-type rat groups for siRNA treatment or UO126 and PI828 treatment, all $SOD1^{G93A}$ and wild-type rats were combined into single $SOD1^{G93A}$ and wild-type groups (i.e., siRNA-treated group and UO126-treated or PI828-treated group) and comparisons between $SOD1^{G93A}$ rats and wild-type littermates were made using a one-way ANOVA. If significant ANOVA differences existed, individual comparisons were made using a Fisher's least-significant difference *post hoc* test (Sigma Plot version 12.0, Systat Software). All differences between groups were considered significant if $p < 0.05$; all values are expressed as means ± 1 SEM.

Results

Phrenic motor neuron survival in end-stage $SOD1^{G93A}$ rats

As shown previously, $SOD1^{G93A}$ rats exhibit phrenic motor neuron cell loss at end stage (Nichols et al., 2013, 2015). We verified putative phrenic motor neuron cell loss at end stage to confirm that the $SOD1^{G93A}$ rats used in this study were similar to those used in previous reports (Fig. 1*A*,*B*). Since there were no significant differences across treatment groups within wild-type or $SOD1^{G93A}$ rats ($p > 0.05$ within wild-type or $SOD1^{G93A}$ groups for siRNA-treated animals or UO126-treated and PI828-treated animals; data not shown), we combined treatment groups into single wild-type versus $SOD1^{G93A}$ groups, and compared putative phrenic motor neuron survival. As shown in Figure 1*C*,*D*, there was significant putative phrenic motor neuron loss in $SOD1^{G93A}$ compared with wild-type rats for siRNA-treated rats as well as for UO126-treated and PI828-treated rats (28 ± 1 and 29 ± 3% survival, respectively; $p < 0.001$). In addition, putative phrenic motor neuron counts in wild-type rats are significantly different for these groups (siRNA-treated rats vs UO126-treated and PI828-treated rats; $p < 0.05$), which likely reflects variability across generations; however, putative phrenic motor neuron survival is not significantly different for $SOD1^{G93A}$ rats (28 ± 1 vs 29 ± 3% survival $p = 0.290$). Thus, putative phrenic motor neuron cell death in this population of $SOD1^{G93A}$ rats is consistent with previously reported studies that used Nissl and/or choline acetyltransferase staining to estimate phrenic motor neuron numbers (Nichols et al., 2013, 2015).

Blood gases

Although there were slight but significant differences within and across groups for $PaCO_2$, it was successfully regulated ±1.5 mmHg of baseline in all groups studied (Table 1; changes >1.5 mmHg of baseline in $PaCO_2$ can influence pLTF; Bach and Mitchell, 1996). Thus, changes in integrated phrenic nerve burst amplitude with time (i.e., pLTF) cannot be attributed to differences in chemoreceptor feedback. PaO_2 and mean arterial pressure significantly decreased during hypoxia in all groups (Table 1). PaO_2 within hypoxic episodes was successfully maintained within the target range (35–45 mmHg; Table 1). We suggest that significant differences across groups for baseline PaO_2 were probably not biologically relevant since PaO_2 was maintained above 150 mmHg at baseline and 60 min after AIH (Table 1). Slight but significant mean arterial pressure differences within groups were <20 mmHg after hypoxia, and were consistent among groups (Table 1). Changes in mean arterial pressure of ≤20 mmHg from control values have minimal effect on respiratory activity in rats (Walker and Jennings, 1995; Bach and Mitchell, 1996). Thus, differences in $PaCO_2$, PaO_2, or mean arterial pressure regulation among groups cannot account for differential pLTF responses.

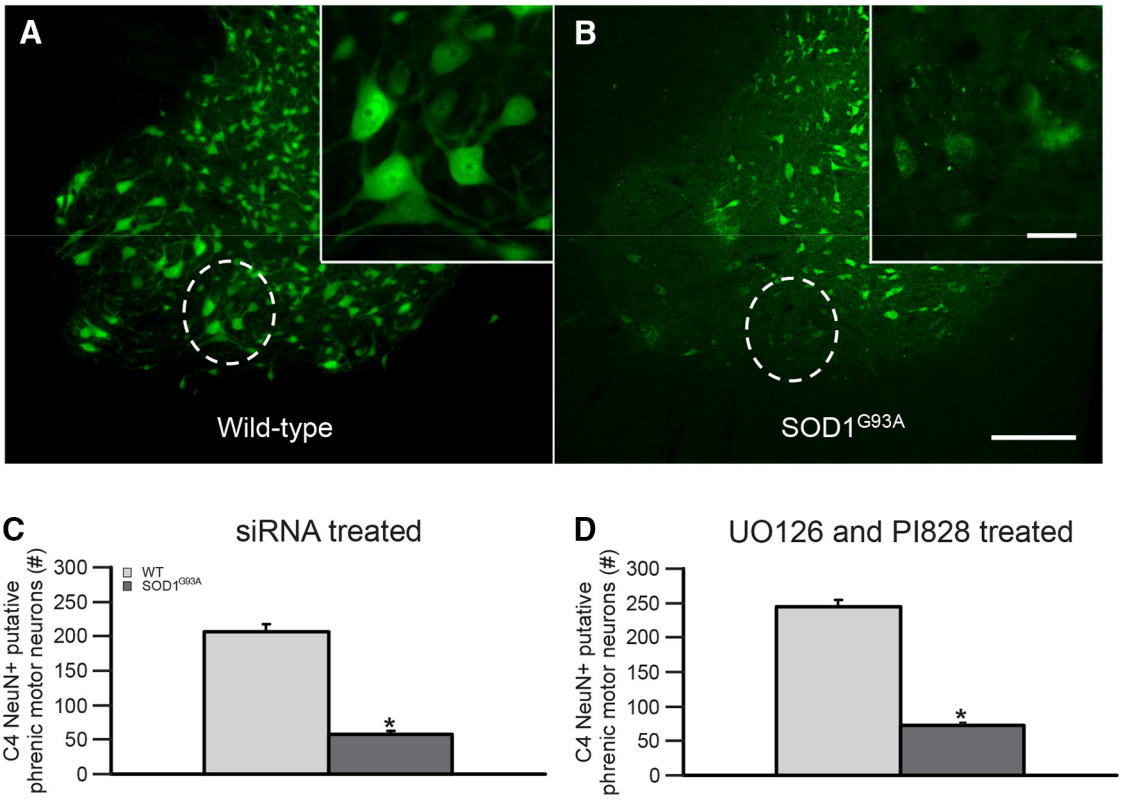

Figure 1. Phrenic motor neuron survival at end stage in *SOD1*^{G93A} rats. ***A***, ***B***, Photomicrographs of NeuN staining (green) in putative phrenic motor neurons from an end-stage *SOD1*^{G93A} rat (***B***) and wild-type littermate (***A***). The phrenic motor nucleus is circumscribed in each panel, and is shown at higher magnification in the inset in each panel. ***C***, ***D***, Number of surviving C4 NeuN+ putative phrenic motor neurons were counted and compared between siRNA-treated (***C***) and UO126-treated and PI828-treated (***D***) *SOD1*^{G93A} rats (dark gray bars) compared with wild-type (WT) littermates (light gray bars). Phrenic motor neuron counts were lower in *SOD1*^{G93A} rates compared with age-matched WT rats (*$p < 0.001$). Scale bars: (in ***B***) ***A***, ***B***, 200 μm; higher-magnification insets (in ***B***) ***A***, ***B***, 50 μm. Values are means ± 1 SEM.

Table 1. Arterial PCO_2, PO_2 and mean arterial pressure during baseline, the first hypoxic episode, and 60 min following AIH in end-stage *SOD1*^{G93A} rats and wild-type littermates

	P_{aCO2} (mmHg)			P_{aO2} (mmHg)			Mean arterial pressure (mmHg)		
Experimental groups	Baseline	Hypoxia	60 min	Baseline	Hypoxia	60 min	Baseline	Hypoxia	60 min
With AIH									
siNT									
Wild-type	52.5 ± 1.5	52.6 ± 1.6	52.5 ± 1.8	325 ± 5^{a,b,f}	40.7 ± 1.0^{g}	296 ± 19^{a,f}	116 ± 9^{a}	75 ± 8^{f,g}	111 ± 8^{a,f}
SOD1^{G93A}	51.0 ± 1.8^{a}	52.5 ± 2.0	51.5 ± 1.5	334 ± 8^{a}	42.6 ± 2.2^{h}	325 ± 9^{a}	98 ± 7^{a}	71 ± 6^{h}	95 ± 7^{a}
siBDNF									
Wild-type	52.5 ± 1.6	51.7 ± 1.8	53.0 ± 1.7^{a}	313 ± 9^{a,f}	38.8 ± 0.8^{g}	304 ± 7^{a,f}	112 ± 6^{a,b}	65 ± 4^{g}	99 ± 6^{a}
SOD1^{G93A}	51.2 ± 0.6	50.8 ± 0.7	51.2 ± 0.9	329 ± 4^{a}	40.5 ± 0.6^{h}	316 ± 7^{a}	112 ± 8^{a}	71 ± 7^{h}	100 ± 8^{a}
siTrkB									
Wild-type	54.1 ± 1.7	54.3 ± 1.6	54.5 ± 1.8	299 ± 20^{a,f}	37.5 ± 1.0^{g}	285 ± 20^{a,f}	117 ± 4^{a}	72 ± 4^{f,g}	108 ± 4^{a}
SOD1^{G93A}	52.8 ± 1.5	52.4 ± 1.4	52.7 ± 1.9	318 ± 8^{a}	38.1 ± 1.4^{h}	290 ± 13^{a}	92 ± 21^{a,b}	67 ± 12^{h}	85 ± 12^{a}
Vehicle									
Wild-type	50.9 ± 1.5^{a}	49.7 ± 1.5^{d}	51.3 ± 1.5^{a}	292 ± 9^{a,f}	37.4 ± 1.3^{g}	267 ± 15^{a,f}	98 ± 6^{a,d}	58 ± 8^{g,j}	92 ± 6^{a,d,j}
SOD1^{G93A}	50.6 ± 1.8	50.7 ± 1.8	50.9 ± 2.0	308 ± 12^{a}	36.6 ± 1.2^{h}	293 ± 15^{a}	97 ± 4^{a,b,h}	56 ± 5^{h}	77 ± 5^{a,h,i}
UO126									
Wild-type	48.8 ± 1.0^{d}	48.5 ± 1.3^{d}	49.0 ± 1.0^{d}	303 ± 8^{a,b,f}	37.1 ± 2^{g}	272 ± 18^{a,f}	99 ± 5^{a,b,d}	70 ± 11^{f,g}	84 ± 3^{a,d,j}
SOD1^{G93A}	49.9 ± 1.4	49.4 ± 1.5	49.7 ± 1.3	285 ± 16^{a,e}	39.2 ± 1.9^{h}	271 ± 16^{a,e}	97 ± 3^{a,b}	53 ± 5^{h}	78 ± 8^{a,h,i}
PI828									
Wild-type	51.4 ± 1.2^{a}	49.9 ± 1.4^{d}	51.2 ± 1.0^{a}	230 ± 21^{a}	36.8 ± 1.3^{g}	220 ± 19^{a,g}	106 ± 4^{a,b}	50 ± 4^{g}	88 ± 3^{a,d}
SOD1^{G93A}	51.6 ± 2.0	51.2 ± 1.8	52.2 ± 2.1^{a}	292 ± 20^{a,b,f}	38.3 ± 1.5^{h}	256 ± 25^{a,e,f,h,i}	94 ± 5^{a,b}	54 ± 4^{h}	82 ± 4^{a}
Without AIH (TCs)									
Wild-type	50.0 ± 0.9	49.9 ± 1.0^{d}	50.2 ± 0.8^{d}	297 ± 14^{f}	295 ± 15	282 ± 17	105 ± 4	104 ± 4	98 ± 4^{c}
SOD1^{G93A}	49.7 ± 1.4	49.7 ± 1.6	48.8 ± 1.5^{a,c}	316 ± 8	305 ± 13	299 ± 10	112 ± 5^{a,b}	108 ± 5	95 ± 4

Data are for rats with AIH or without AIH. Rats received intrathecal injections of either (1) siRNAs targeting BDNF (siBDNF), TrkB (siTrkB), or nontarget (siNT) mRNA; or (2) vehicle or inhibitors for MEK/ERK (UO126) or PI3K/Akt (PI828). Significant differences within individual study groups are indicated as follows: ^{a}significant difference from hypoxia, ^{b}significant difference from 60 min, and ^{c}significant difference from baseline. Significant differences across study groups are indicated as follows: ^{d}significant difference from wild-type siTrkB, ^{e}significant difference from *SOD1*^{G93A} siNT, ^{f}significant difference from wild-type PI828, ^{g}significant difference from wild-type without AIH, ^{h}significant difference from *SOD1*^{G93A} without AIH, ^{i}significant difference from *SOD1*^{G93A} siBDNF, and ^{j}significant difference from wild-type siNT. Values are expressed as means ± 1 SEM. Differences were considered significant if $p < 0.05$.

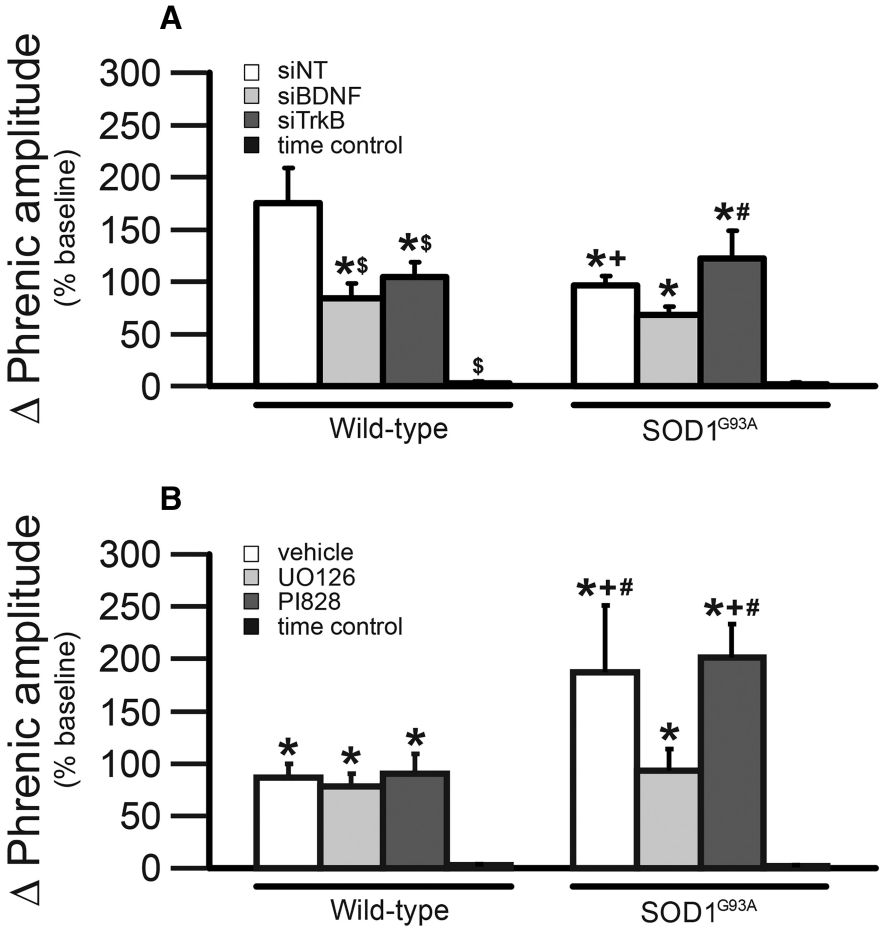

Figure 2. Phrenic response during hypoxia in end-stage *SOD1*^{G93A} rats and age-matched, wild-type littermates. Since phrenic burst amplitude was not different among hypoxic episodes within groups ($p > 0.05$; data not shown), all three episodes were grouped for comparisons across treatment groups. ***A***, White bars represent rats pretreated with siNT; light gray bars represent rats pretreated with siBDNF; dark gray bars represent rats treated with siTrkB; black bars represent TC rats (without hypoxia). Wild-type rats are represented on the left, and *SOD1*^{G93A} rats on the right. Wild-type rats pretreated with siNT had a significantly greater hypoxic phrenic response compared with other wild-type treated rats ($), and with siNT-treated *SOD1*^{G93A} rats (+). *SOD1*^{G93A} rats pretreated with siTrkB had significantly greater hypoxic phrenic responses compared with siBDNF-treated *SOD1*^{G93A} rats (#). Both wild-type and SOD1 ^{G93A} TCs had a smaller phrenic burst amplitude compared with all other (AIH-treated) rats (*). ***B***, White bars represent rats pretreated with vehicle; light gray bars represent rats pretreated with UO126; dark gray bars represent rats treated with PI828; and black bars represent TCs. Wild-type rats are on the left and *SOD1*^{G93A} rats on the right. *SOD1*^{G93A} rats pretreated with vehicle or PI828 had significantly greater hypoxic phrenic responses compared with UO126-treated *SOD1*^{G93A} (#) and wild-type rats (+). Both wild-type and SOD1 ^{G93A} TCs (no AIH) had significantly lower phrenic responses compared with other groups (*). Values are means ± 1 SEM and all significant differences are $p < 0.05$.

Hypoxic response in end-stage *SOD1*^{G93A} rats compared with wild-type littermates

Since short-term hypoxic phrenic responses (episode 1 vs 2 vs 3) were not different from each other ($p > 0.05$; data not shown), they were grouped and compared across treatments (Fig. 2). The hypoxic phrenic response was significantly larger in wild-type rats treated with siNT compared with all other wild-type rats ($p < 0.05$; Fig. 2*A*). Within siRNA-treated *SOD1*^{G93A} rats, the hypoxic phrenic response was significantly larger in siTrkB-treated rats compared with siBDNF-treated *SOD1*^{G93A} rats ($p < 0.05$; Fig. 2*A*). As shown in Figure 2*B*, the hypoxic phrenic response was significantly larger in *SOD1*^{G93A} rats treated with vehicle or PI828 compared with the hypoxic phrenic response of all other rats ($p < 0.05$; Fig. 2*B*). Thus, it is possible that the larger hypoxic phrenic response in *SOD1*^{G93A} rats treated with siTrkB, vehicle, or PI828 may be associated with enhanced pLTF since the magnitude of the hypoxic phrenic response correlates with pLTF in normal rats (Fuller et al., 2000; Baker-Herman and Mitchell, 2008); a similar association occurs with severe AIH-induced (S pathway) pLTF, where larger hypoxic responses and pLTF are observed (Nichols et al., 2012).

pLTF in end-stage *SOD1*^{G93A} rats requires new BDNF and not TrkB synthesis

One goal of this study was to investigate mechanisms responsible for pLTF in *SOD1*^{G93A} rats with differential treatments known to intervene in either the Q or S pathway to pMF. Thus, we delivered intrathecal siBDNF and siTrkB to disrupt the Q and S pathways, respectively. Representative phrenic neurograms are shown for AIH-exposed *SOD1*^{G93A} rats ~2 h after intrathecal delivery of nontargeting siRNA (siNT; Fig. 3*A*) or siRNAs targeting BDNF (siBDNF; Fig. 3*B*) or TrkB (siTrkB; Fig. 3*C*) mRNA. pLTF was significantly greater in wild-type and *SOD1*^{G93A} rats treated with siTrkB or siNT compared with baseline, siBDNF-treated rats, and TCs (all p's < 0.05; Figs. 3*D*,*E*). Thus, pLTF in both end-stage *SOD1*^{G93A} and wild-type rats requires new BDNF synthesis versus new synthesis of TrkB, consistent with the Q pathway to pMF.

pLTF in end-stage *SOD1*^{G93A} rats requires MEK/ERK and not PI3K/Akt activity

To further confirm Q-pathway versus S-pathway involvement for pLTF of *SOD1*^{G93A} rats, we delivered the MEK inhibitor UO126 to inhibit ERK phosphorylation, and the PI3 kinase inhibitor PI828 to inhibit the phosphorylation of Akt. Representative phrenic neurograms are shown for *SOD1*^{G93A} rats exposed to AIH ~20 min after intrathecal delivery of vehicle (Fig. 4*A*), UO126 (Fig. 4*B*), or PI828 (Fig. 4*C*). pLTF was significantly greater in wild-type and *SOD1*^{G93A} rats treated with vehicle or PI828 compared with rats treated with UO126 or with TCs (both p's < 0.05; Fig. 4*D*,*E*). pLTF in UO126-treated wild-type and *SOD1*^{G93A} rats was not significantly different from that of TCs, leading us to conclude that pLTF in end-stage *SOD1*^{G93A} and wild-type rats requires MEK/ERK, and not PI3K/Akt, activity. This result is again consistent with the interpretation that enhanced pLTF in *SOD1*^{G93A} rats results from an enhanced Q pathway, without evidence for increased S-pathway contributions.

Frequency LTF

In this experimental preparation, AIH-induced frequency LTF is inconsistent and small (but significant) compared with burst amplitude LTF (i.e., pLTF; Baker-Herman and Mitchell, 2008). After AIH, burst frequency was significantly greater in wild-type rats treated with siBDNF or siNT compared with baseline and TCs (all p's < 0.05; Fig. 5*A*). Frequency LTF was observed in *SOD1*^{G93A} rats treated with siBDNF, siTrkB, and siNT versus baseline and TCs (all p's < 0.05; Fig. 5*B*). Similarly, burst fre-

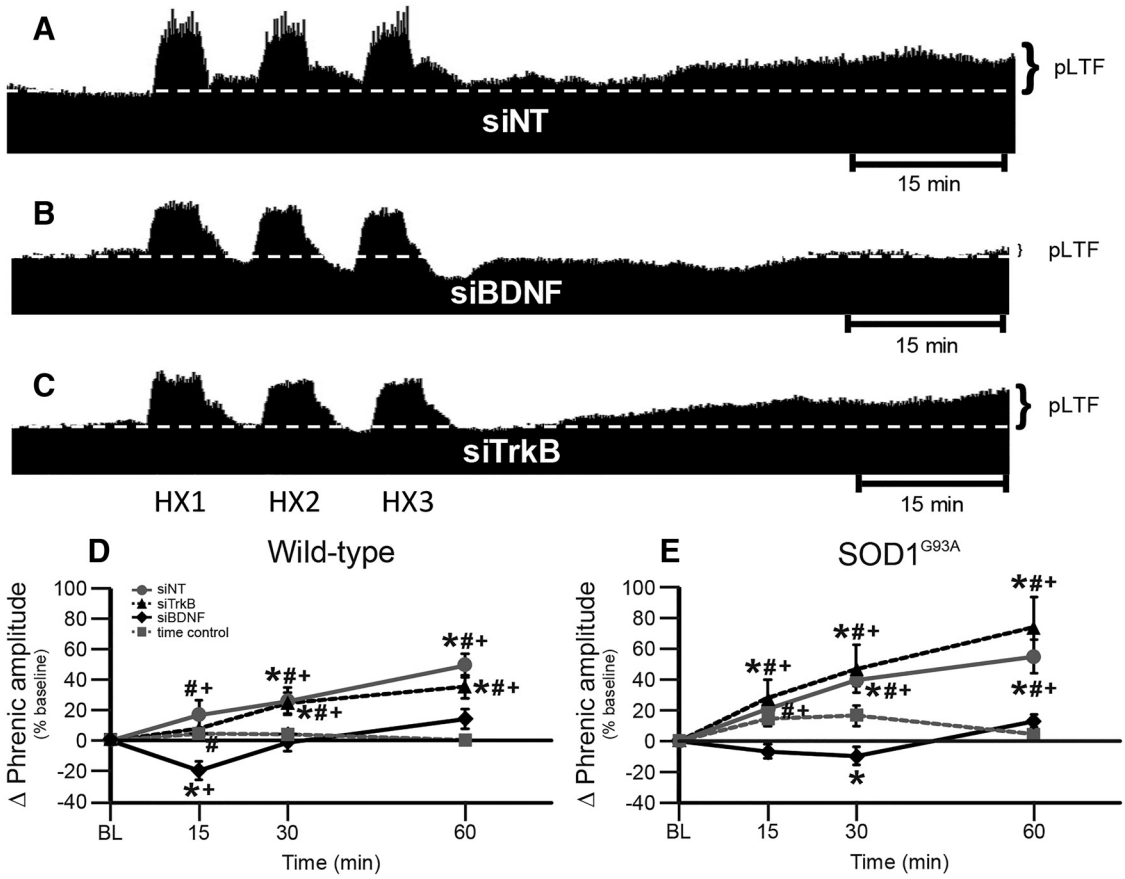

Figure 3. pLTF in siRNA-treated rats. ***A–C***, Representative traces of compressed, integrated phrenic nerve activity before and after AIH in end-stage *SOD1*^{G93A} rats pretreated with siNT (***A***), siBDNF (***B***), or siTrkB (***C***). White, dashed line in each trace indicates baseline. AIH elicits pLTF in siNT-pretreated and siTrkB-pretreated rats, but was nearly abolished in siBDNF-pretreated rats. ***D***, ***E***, Phrenic burst amplitude (percentage change from baseline) in wild-type (***D***) and *SOD1*^{G93A} (***E***) rats pretreated with siNT (gray circles with gray solid line), siTrkB (black triangles with black dashed line), or siBDNF (black diamonds with black solid line), or TCs (gray squares with gray dashed line). pLTF is significantly increased in wild-type and *SOD1*^{G93A} rats treated with siNT or siTrkB compared with baseline (+) and with TCs (*), indicating pLTF. Wild-type and *SOD1*^{G93A} rats treated with siBDNF had a significantly smaller pLTF compared with baseline (+) or with TCs (*; at only 15 min after hypoxia for wild type and only 30 min after hypoxia for *SOD1*^{G93A}) and with siNT-treated or siTrkB-treated rats (#; all time points after hypoxia). Values are means ± 1 SEM and all significant differences are $p < 0.05$.

quency was significantly greater in wild-type and *SOD1*^{G93A} rats treated with vehicle or PI828 compared with baseline burst frequency and burst frequency of TCs ($p < 0.05$; Fig. 5*C*,*D*). In *SOD1*^{G93A} rats treated with vehicle or PI828, frequency LTF was significantly larger than in *SOD1*^{G93A} rats treated with UO126 at all times ($p < 0.05$; Fig. 5*D*). Thus, we report that both wild-type and *SOD1*^{G93A} rats exhibit small frequency LTF, as described previously (Baker-Herman and Mitchell, 2008); in contrast to what has been reported in naive rats (Hoffman et al., 2012), mAIH-induced frequency LTF is similarly abolished by MEK/ERK inhibition, but not by inhibition of BDNF synthesis. However, the differences observed here are small.

Phrenic motor neuron BDNF and pERK expression are increased in *SOD1*^{G93A} rats

Since the Q pathway is the dominant mechanism contributing to pLTF in normal rats following moderate AIH, and the Q pathway requires BDNF synthesis and ERK phosphorylation, we hypothesized that these same proteins would be upregulated in spared phrenic motor neurons in *SOD1*^{G93A} versus wild-type rats (Fig. 6). Representative photomicrographs for BDNF and pERK immunoreactivity in putative phrenic motor neurons from *SOD1*^{G93A} and wild-type rats are shown in Figure 6*A*,*B*,*D*,*E*. In *SOD1*^{G93A} rats, BDNF and pERK expression in surviving putative phrenic motor neurons was significantly greater in *SOD1*^{G93A} rats than in wild-type littermates ($p < 0.05$; Fig. 6*C*,*F*). Increased phrenic motor neuron BDNF and pERK expression in *SOD1*^{G93A} rats is consistent with enhancement of the Q pathway to pMF.

Discussion

We report that in end-stage *SOD1*^{G93A} rats (1) phrenic motor neuron survival is similar to previous reports from our group in this same experimental model (Nichols et al., 2013, 2015), (2) BDNF and pERK protein expression are increased in spared putative phrenic motor neurons, and (3) moderate AIH-induced pLTF still requires new BDNF synthesis and MEK/ERK signaling, but not TrkB synthesis or PI3K/Akt signaling. We conclude that pLTF following moderate AIH results from augmentation of normal pLTF mechanisms (i.e., the Q pathway; Dale-Nagle et al., 2010) rather than additional contributions from alternate mechanisms (such as the S pathway). These findings have profound implications concerning the ability to harness moderate AIH to increase endogenous function of the underlying mechanisms responsible for pLTF, and to preserve/restore breathing capacity with ALS disease progression.

New BDNF synthesis is required for pLTF in *SOD1*^{G93A} rats

The Q and S pathways are each capable of eliciting pMF and pLTF in normal rats when acting alone; the Q pathway dominates with

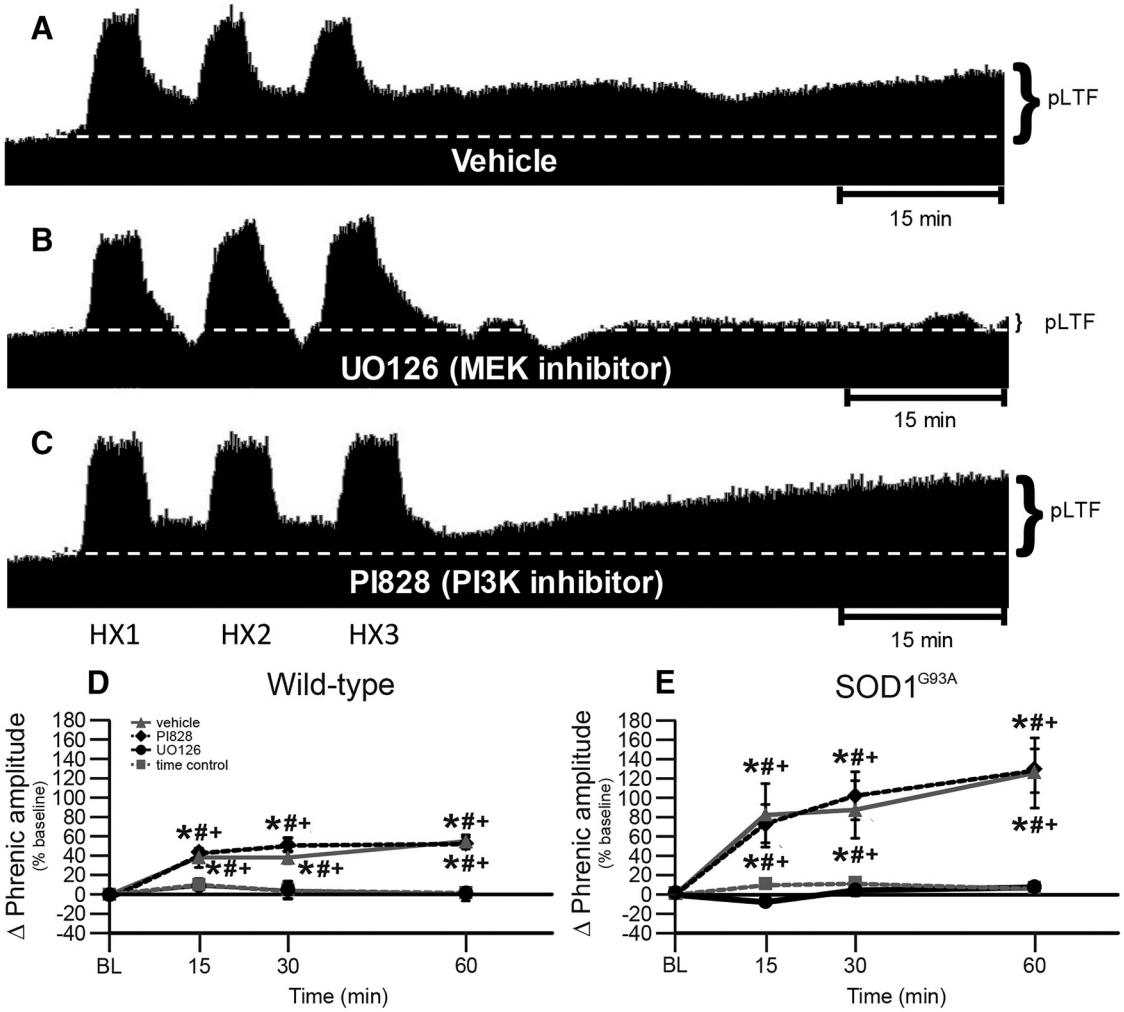

Figure 4. pLTF in UO126-treated and PI828-treated rats. ***A–C***, Representative traces of compressed, integrated phrenic nerve activity before and after AIH in end-stage $SOD1^{G93A}$ rats pretreated with vehicle (***A***), UO126 (***B***), or PI828 (***C***). White dashed line in each trace indicates baseline. AIH elicits pLTF in vehicle-pretreated and PI828-pretreated rats, but was nearly abolished in UO126-pretreated rats. ***D***, ***E***, Phrenic burst amplitude (percentage change from baseline) in wild-type (***D***) and $SOD1^{G93A}$ (***E***) rats pretreated with vehicle (gray triangles with gray solid line), PI828 (black diamonds with black dashed line), or UO126 (black circles with black solid line), or TCs (gray squares with gray dashed line). pLTF is increased in wild-type and $SOD1^{G93A}$ rats treated with vehicle or PI828 compared with baseline (+) and with TCs (*). Wild-type and $SOD1^{G93A}$ rats treated with UO126 had a significantly smaller pLTF compared with vehicle or with PI828 (#). Values are means ± 1 SEM; significant differences are $p < 0.05$.

moderate AIH (Dale-Nagle et al., 2010; Devinney et al., 2013), whereas the S pathway dominates with severe AIH (Nichols et al., 2012). Here we tested the idea that the S pathway may be recruited to enhance pLTF in end-stage $SOD1^{G93A}$ rats. In contrast, we found that pLTF following moderate AIH results from enhanced Q-pathway contributions.

Both the Q (Baker-Herman and Mitchell, 2002) and the S pathways (Golder et al., 2008) require new protein synthesis, but a major distinguishing feature is the reliance on new synthesis of BDNF (Q; Baker-Herman et al., 2004) rather than TrkB (S; Golder et al., 2008; Hoffman et al., 2012). Since siBDNF, and not siTrkB, abolishes moderate AIH-induced pLTF in both wild-type and end-stage $SOD1^{G93A}$ rats, we conclude that pLTF remains Q-pathway dependent (Figs. 3, 7).

BDNF is increased in astrocytes and microglia within the phrenic motor nucleus of end-stage $SOD1^{G93A}$ rats (Satriotomo et al., 2006), and we now show that BDNF expression is increased in putative phrenic motor neurons in end-stage $SOD1^{G93A}$ rats (Fig. 6). This increase in motor neuron BDNF expression is consistent with enhanced BDNF function in end-stage $SOD1^{G93A}$ rats. Mechanisms amplifying basal BDNF protein levels in end-stage $SOD1^{G93A}$ rats remain unknown.

MEK/ERK signaling is required for pLTF in $SOD1^{G93A}$ rats

Another distinguishing feature between the Q-pathway versus S-pathway contributions to AIH-induced pLTF is the reliance on MEK/ERK (Q) versus PI3 kinase/Akt (S) signaling (Dale-Nagle et al., 2010). ERK expression is increased in the phrenic motor nucleus after repetitive AIH exposure (Wilkerson and Mitchell, 2009; Satriotomo et al., 2012), and increased expression may enhance phrenic motor plasticity (Wilkerson and Mitchell, 2009). Here we show that pERK expression in spared putative phrenic motor neurons in end-stage $SOD1^{G93A}$ rats is increased (Fig. 6). Further, since MEK/ERK inhibition with UO126, but not PI3K/Akt inhibition with PI828, blocked pLTF in both wild-type and $SOD1^{G93A}$ rats (Figs. 4, 7), we suggest that pLTF arises from enhanced Q-pathway contributions, and does not require additional S-pathway contributions.

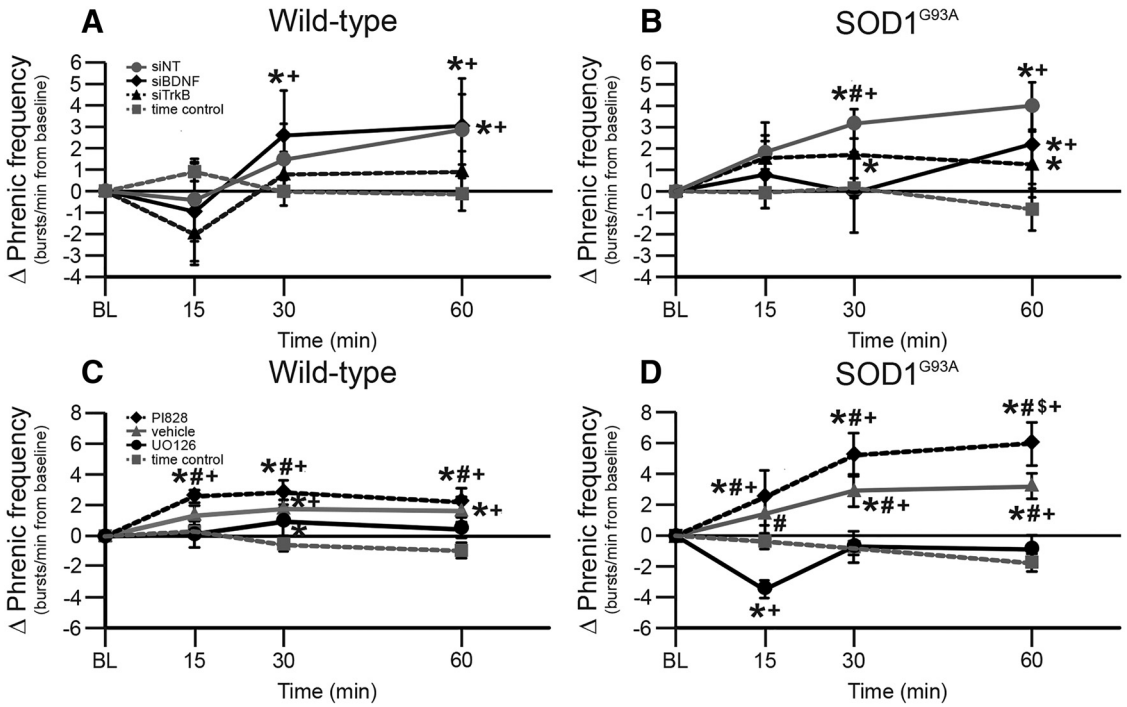

Figure 5. Burst frequency response in end-stage *SOD1*^{G93A} and wild-type rats. ***A***, ***B***, Burst frequency response (change from baseline, bursts/min) in wild-type (***A***) and *SOD1*^{G93A} (***B***) rats pretreated with siNT (gray circles with solid gray line), siTrkB (black triangles with black dashed line), or siBDNF (black diamonds with solid black line), or TCs (gray squares with gray dashed line). In ***A***, burst frequency is significantly increased in wild-type rats treated with siNT or siBDNF compared with baseline (+) and with TCs (*). In ***B***, burst frequency is significantly increased in *SOD1*^{G93A} rats treated with siNT, siTrkB, or siBDNF compared with baseline (+) and with TCs (*). *SOD1*^{G93A} rats treated with siBDNF had smaller burst frequencies compared with rats treated with siNT (#; at 30 min after hypoxia). ***C***, ***D***, Burst frequency response in wild-type (***C***) and *SOD1*^{G93A} (***D***) rats pretreated with vehicle (gray triangles with solid gray line), PI828 (black diamonds with black dashed line), or UO126 (black circles with black solid line), or TCs (gray squares with gray dashed line). In ***C***, burst frequency is significantly increased in wild-type rats treated with PI828, vehicle, or UO126 compared with baseline (+) and with TCs (*). UO126-treated wild-type rats had a significantly smaller burst frequency compared with PI828-treated rats (#). In ***D***, burst frequency is significantly increased in *SOD1*^{G93A} rats treated with PI828 or vehicle compared with baseline (+) and with TCs (*). UO126-treated *SOD1*^{G93A} rats had a significantly smaller burst frequency compared with PI828 (#), with vehicle (#), with baseline (+; at 15 min posthypoxia), and with TCs (*; at 15 min posthypoxia). PI828-treated *SOD1*^{G93A} rats also had a larger burst frequency compared with vehicle-treated rats ($; at 60 min posthypoxia). Values are means ± 1 SEM; significant differences are $p < 0.05$.

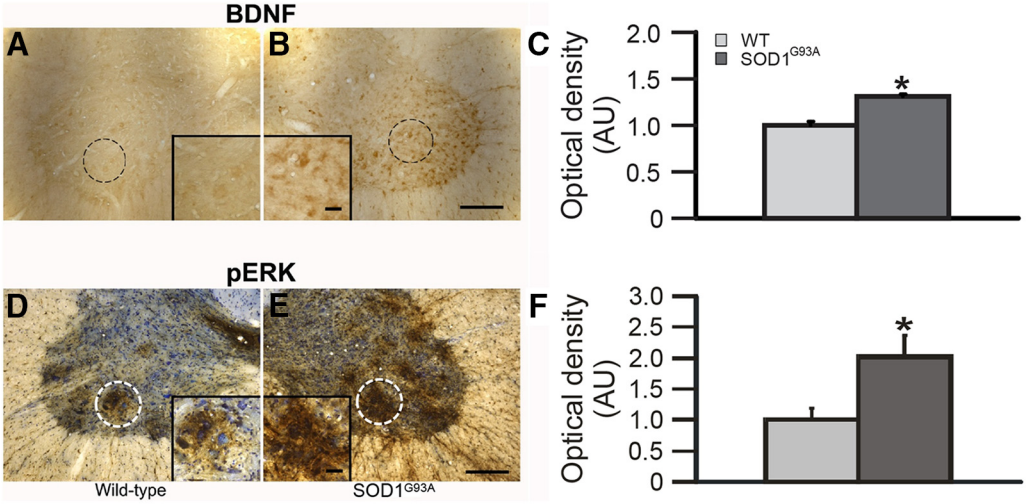

Figure 6. ***A–F***, BDNF (***A–C***) and pERK (***D–F***) expression in putative phrenic motor neurons. Representative BDNF (***A***, ***B***) and pERK (***D***, ***E***) immunostaining in putative C4 phrenic motor neurons from wild-type (***A***, ***D***) and *SOD1*^{G93A} (***B***, ***E***) rats; BDNF and pERK immunostaining are a brown reaction product. In ***D*** and ***E***, neurons were counterstained with cresyl-violet (blue). The putative phrenic motor nucleus is circumscribed in ***A***, ***B***, ***D***, and ***E***, shown at higher magnification in insets. Densitometry was performed within these circumscribed areas. OD measurements demonstrated significant increases in BDNF (***C***) and pERK (***F***) expression in the putative phrenic motor nucleus of *SOD1*^{G93A} (dark gray bar) rats compared with wild-type (WT; light gray bar) littermates. Values are means ± 1 SEM. *$p < 0.05$ versus wild-type rats. Scale bars: low magnification, 200 μm; high magnification, 50 μm.

Enhanced plasticity does not result from differential phrenic motor neuron death

In *SOD1*^{G93A} rats, the age at end stage can drift due to an unstable copy number (Suzuki et al., 2007). Thus, equivalent phrenic motor neuron cell death must be verified in each generation to ensure consistent motor neuron degeneration. Indeed, phrenic motor neuron death/survival was comparable across all treatment groups (Fig. 1; Nichols et al., 2013, 2015). Thus, enhanced moderate AIH-induced

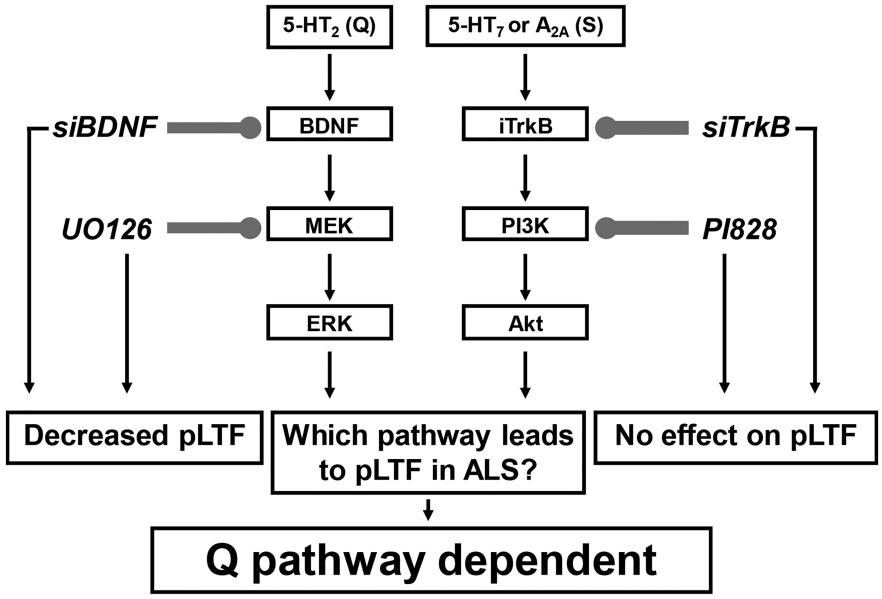

Figure 7. Working model of enhanced phrenic pLTF in end-stage *SOD1*^{G93A} rats. pLTF is regulated by G_q-protein-coupled (5-HT_2) or G_s-protein-coupled (5-HT_7 and A_{2A}) metabotropic receptors (activating the Q and S pathways, respectively). We speculate that 5-HT_2 receptor activation induces new BDNF synthesis and MEK/ERK activation, whereas 5-HT_7 or A_{2A} receptor activation induces new TrkB synthesis and PI3K/Akt activation. Either mechanism acting alone can produce pLTF in normal rats. Both intrathecal siBDNF (targeting BDNF mRNA) and UO126 (MEK/ERK inhibitor) blocked pLTF in wild-type and *SOD1*^{G93A} rats, confirming that the predominant mechanism of pLTF is the Q pathway. In contrast, intrathecal siTrkB (targeting TrkB mRNA) or PI828 (PI3K/Akt inhibitor) failed to block moderate AIH-induced pLTF in *SOD1*^{G93A} or wild-type rats, demonstrating that the S pathway does not contribute to pLTF in *SOD1*^{G93A} or wild-type rats. Thus, enhanced pLTF in *SOD1*^{G93A} rats arises from increased Q-pathway contributions.

pLTF in end-stage *SOD1*^{G93A} rats resulted from increased plasticity in spared phrenic motor neurons rather than from differential motor neuron survival.

Increased Q-pathway contributions enhance phrenic plasticity in other models

Enhanced moderate AIH-induced pLTF has been observed in a number of models, including cervical dorsal rhizotomy (Kinkead et al., 1998), pretreatment with chronic intermittent hypoxia (Ling et al., 2001; Fuller et al., 2003; McGuire et al., 2003, 2004; Peng and Prabhakar, 2004), and pretreatment with daily AIH (Wilkerson and Mitchell, 2009). However, somewhat different mechanisms appear to enhance phrenic motor plasticity in these various models. For example, enhanced pLTF following cervical dorsal rhizotomy relies on enhanced Q-pathway contributions since enhanced pLTF is blocked by systemic administration of the 5HT_{2A} receptor (Q pathway) antagonist ketanserin (Kinkead et al., 1998). In contrast, in rats pretreated with chronic intermittent hypoxia (Ling et al., 2001; McGuire et al., 2004), both the Q and S pathways may contribute to enhanced plasticity (Fields and Mitchell, 2015). Following 1 week of chronic intermittent hypoxia, ketanserin only partially blocked enhanced pLTF, whereas the nonselective antagonists methysergide (broad spectrum) and clozapine (5$HT_{2,6,7}$ antagonist) abolished enhanced LTF (Ling et al., 2001; McGuire et al., 2004). Enhanced moderate AIH-induced pLTF following chronic intermittent hypoxia may require increased contributions from a distinct 5HT receptor, likely 5HT_7 receptors (Ling et al., 2001; McGuire et al., 2004). Since 5-HT7 receptors are G_s-protein-coupled, they represent a form of S-pathway contribution to pMF (Hoffman and Mitchell, 2011; 2013). In agreement, pretreatment with daily AIH for 7 d (10 5 min episodes of hypoxia, 5 min normoxic intervals) increases ventral cervical BDNF protein levels, but a single AIH presentation no longer increases BDNF from that increased basal level (Wilkerson and Mitchell, 2009). Although the functional significance of elevated BDNF protein levels is not clear, increased basal BDNF levels may enable pLTF without new protein synthesis (Wilkerson and Mitchell, 2009). Observations here suggest that new BDNF synthesis remains essential for pLTF (Fig. 3) despite increased phrenic motor neuron BDNF levels in end-stage disease (Fig. 6). Thus, mechanisms enhancing pLTF in end-stage motor neuron disease are similar to enhanced pLTF following cervical dorsal rhizotomy (i.e., Q-pathway-dependent; Kinkead et al., 1998), but contrasts with mechanisms of enhanced pLTF after chronic intermittent hypoxia preconditioning, where both Q-pathway (5-HT2) and S-pathway (5-HT7) contributions appear to be involved (Ling et al., 2001; McGuire et al., 2004).

Significance

This study increases our understanding of induced respiratory motor plasticity and metaplasticity (Mitchell and Johnson, 2003; Fields and Mitchell, 2015), and the potential to harness plasticity as a means of preserving or restoring breathing capacity during motor neuron disease progression. In this respect, AIH (i.e., pLTF) may represent an interesting new treatment modality for ALS patients, just as it has been used to successfully "treat" rodent models (Lovett-Barr et al., 2012; Navarrete-Opazo et al., 2015, 2017a) and patients with chronic, incomplete spinal injury (Trumbower et al., 2012; Hayes et al., 2014; Navarrete-Opazo et al., 2017b). In specific, rodent models of cervical spinal injury (Lovett-Barr et al., 2012; Navarrete-Opazo et al., 2015, 2017a) and humans with chronic spinal injury (Tester et al., 2014) exhibit greater breathing following daily AIH. AIH has also improved walking ability in rodents (Lovett-Barr et al., 2012; Prosser-Loose et al., 2015) and in humans with chronic, incomplete spinal injuries (Trumbower et al., 2012; Hayes et al., 2014; Navarrete-Opazo et al., 2017b). However, the impact of repetitive AIH on nonrespiratory somatic motor function in ALS has not been investigated (Mitchell, 2007; Dale et al., 2014).

Harnessing the potential for AIH-induced respiratory motor plasticity may preserve and/or restore lost breathing capacity in ALS patients, delaying ventilator dependence and improving the quality of life for individuals afflicted with this devastating, progressive disorder. Our ever-expanding knowledge concerning cellular mechanisms of AIH-induced respiratory motor plasticity may suggest new targets to preserve/restore respiratory motor function through pharmacological or gene-therapy approaches, possibly targeting BDNF/TrkB and/or MEK/ERK signaling.

References

Bach KB, Mitchell GS (1996) Hypoxia-induced long-term facilitation of respiratory activity is serotonin dependent. Respir Physiol 104:251–260. CrossRef Medline

Baker TL, Mitchell GS (2000) Episodic but not continuous hypoxia elicits

long-term facilitation of phrenic motor output in rats. J Physiol 529:215–219. CrossRef Medline

Baker-Herman TL, Mitchell GS (2002) Phrenic long-term facilitation requires spinal serotonin receptor activation and protein synthesis. J Neurosci 22:6239–6246. Medline

Baker-Herman TL, Mitchell GS (2008) Determinants of frequency long-term facilitation following acute intermittent hypoxia in vagotomized rats. Respir Physiol Neurobiol 162:8–17. CrossRef Medline

Baker-Herman TL, Fuller DD, Bavis RW, Zabka AG, Golder FJ, Doperalski NJ, Johnson RA, Watters JJ, Mitchell GS (2004) BDNF is necessary and sufficient for spinal respiratory plasticity following intermittent hypoxia. Nat Neurosci 7:48–55. CrossRef Medline

Boulenguez P, Gestreau C, Vinit S, Stamegna JC, Kastner A, Gauthier P (2007) Specific and artifactual labeling in the rat spinal cord and medulla after injection of monosynaptic retrograde tracers into the diaphragm. Neurosci Lett 417:206–211. CrossRef Medline

Bourke SC, Shaw PJ, Gibson GJ (2001) Respiratory function vs sleep-disordered breathing as predictors of QOL in ALS. Neurology 57:2040–2044. CrossRef Medline

Dale EA, Satriotomo I, Mitchell GS (2012) Cervical spinal erythropoietin induces phrenic motor facilitation via extracellular signal-regulated protein kinase and Akt signaling. J Neurosci 32:5973–5983. CrossRef Medline

Dale EA, Ben Mabrouk F, Mitchell GS (2014) Unexpected benefits of intermittent hypoxia: enhanced respiratory and nonrespiratory motor function. Physiology 29:39–48. CrossRef Medline

Dale-Nagle EA, Hoffman MS, MacFarlane PM, Mitchell GS (2010) Multiple pathways to long-lasting phrenic motor facilitation. Adv Exp Med Biol 669:225–230. CrossRef Medline

Dale-Nagle EA, Satriotomo I, Mitchell GS (2011) Spinal vascular endothelial growth factor induces phrenic motor facilitation via extracellular signal-regulated kinase and Akt signaling. J Neurosci 31:7682–7690. CrossRef Medline

Devinney MJ, Huxtable AG, Nichols NL, Mitchell GS (2013) Hypoxia-induced phrenic long-term facilitation: emergent properties. Ann N Y Acad Sci 1279:143–153. CrossRef Medline

Feldman JL, Mitchell GS, Nattie EE (2003) Breathing: rhythmicity, plasticity, chemosensitivity. Annu Rev Neurosci 26:239–266. CrossRef Medline

Fields DP, Mitchell GS (2015) Spinal metaplasticity in respiratory motor control. Front Neural Circuits 9:2. CrossRef Medline

Fuller DD, Bach KB, Baker TL, Kinkead R, Mitchell GS (2000) Long term facilitation of phrenic motor output. Respir Physiol 121:135–146. CrossRef Medline

Fuller DD, Johnson SM, Olson EB Jr, Mitchell GS (2003) Synaptic pathways to phrenic motoneurons are enhanced by chronic intermittent hypoxia after cervical spinal cord injury. J Neurosci 23:2993–3000. Medline

Golder FJ, Ranganathan L, Satriotomo I, Hoffman M, Lovett-Barr MR, Watters JJ, Baker-Herman TL, Mitchell GS (2008) Spinal adenosine A2a receptor activation elicits long-lasting phrenic motor facilitation. J Neurosci 28:2033–2042. CrossRef Medline

Gonzalez-Rothi EJ, Lee KZ, Dale EA, Reier PJ, Mitchell GS, Fuller DD (2015) Intermittent hypoxia and neurorehabilitation. J Appl Physiol 119:1455–1465. CrossRef Medline

Gurney ME, Pu H, Chiu AY, Dal Canto MC, Polchow CY, Alexander DD, Caliendo J, Hentati A, Kwon YW, Deng HX, Chen W, Zhai P, Sufit RL, Siddique T (1994) Motor neuron degeneration in mice that express a human Cu, Zn superoxide dismutase mutation. Science 264:1772–1775. CrossRef Medline

Hayes HB, Jayaraman A, Herrmann M, Mitchell GS, Rymer WZ, Trumbower RD (2014) Daily intermittent hypoxia enhances walking after chronic spinal cord injury: a randomized trial. Neurology 82:104–113. CrossRef Medline

Hoffman MS, Mitchell GS (2011) Spinal 5-HT7 receptor activation induces long-lasting phrenic motor facilitation. J Physiol 589:1397–1407. CrossRef Medline

Hoffman MS, Mitchell GS (2013) Spinal 5-HT7 receptors and protein kinase A constrain intermittent hypoxia-induced phrenic long-term facilitation. Neuroscience 250:632–643. CrossRef Medline

Hoffman MS, Nichols NL, Macfarlane PM, Mitchell GS (2012) Phrenic long-term facilitation after acute intermittent hypoxia requires spinal ERK activation but not TrkB synthesis. J Appl Physiol 113:1184–1193. CrossRef Medline

Howland DS, Liu J, She Y, Goad B, Maragakis NJ, Kim B, Erickson J, Kulik J, DeVito L, Psaltis G, DeGennaro LJ, Cleveland DW, Rothstein JD (2002) Focal loss of the glutamate transporter EAAT2 in a transgenic rat model of SOD1 mutant-mediated amyotrophic lateral sclerosis (ALS). Proc Natl Acad Sci U S A 99:1604–1609. CrossRef Medline

Iłzecka J, Stelmasiak Z, Balicka G (2003) Respiratory function in amyotrophic lateral sclerosis. Neurol Sci 24:288–289. CrossRef Medline

Kiernan MC, Vucic S, Cheah BC, Turner MR, Eisen A, Hardiman O, Burrell JR, Zoing MC (2011) Amyotrophic lateral sclerosis. Lancet 377:942–955. CrossRef Medline

Kinkead R, Zhan WZ, Prakash YS, Bach KB, Sieck GC, Mitchell GS (1998) Cervical dorsal rhizotomy enhances serotonergic innervation of phrenic motoneruons and serotonin-dependent long-term facilitation of respiratory motor output in rats. J Neurosci 18:8436–8443. Medline

Lechtzin N, Rothstein J, Clawson L, Diette GB, Wiener CM (2002) Amyotrophic lateral sclerosis: evaluation and treatment of respiratory impairment. Amyotroph Lateral Scler Other Motor Neuron Disord 3:5–13. Medline

Ling L, Fuller DD, Bach KB, Kinkead R, Olson EB Jr, Mitchell GS (2001) Chronic intermittent hypoxia elicits serotonin-dependent plasticity in the central neural control of breathing. J Neurosci 21:5381–5388. Medline

Lovett-Barr MR, Satriotomo I, Muir GD, Wilkerson JE, Hoffman MS, Vinit S, Mitchell GS (2012) Repetitive intermittent hypoxia induces respiratory and somatic motor recovery following chronic cervical spinal injury. J Neurosci 32:3591–3600. CrossRef Medline

Lyall RA, Donaldson N, Polkey MI, Leigh PN, Moxham J (2001) Respiratory muscle strength and ventilatory failure in amyotrophic lateral sclerosis. Brain 124:2000–2013. CrossRef Medline

Mantilla CB, Zhan WZ, Sieck GC (2009) Retrograde labeling of phrenic motoneurons by intrapleural injection. J Neurosci Methods 182:244–249. CrossRef Medline

McGuire M, Zhang Y, White DP, Ling L (2003) Chronic intermittent hypoxia enhances ventilatory long-term facilitation in awake rats. J Appl Physiol 95:1499–1508. CrossRef Medline

McGuire M, Zhang Y, White DP, Ling L (2004) Serotonin receptor subtypes required for ventilatory long-term facilitation and its enhancement after chronic intermittent hypoxia in awake rats. Am J Physiol Regul Integr Comp Physiol 286:R334–R341. CrossRef Medline

Mitchell GS (2007) Respiratory plasticity following intermittent hypoxia: a guide for novel therapeutic approaches to ventilator control disorders. In: Genetic basis for respiratory control disorders (Gaultier C, ed), pp 291–306. New York: Springer.

Mitchell GS, Johnson SM (2003) Neuroplasticity in respiratory motor control. J Appl Physiol 94:358–374. CrossRef Medline

Mitchell GS, Douse MA, Foley KT (1990) Receptor interactions in modulating ventilatory activity. Am J Physiol 259:R911–R920. Medline

Mitchell GS, McCrimmon DR, Feldman JL, Baker-Herman TL (2009) Respiration. In: Encyclopedia of neuroscience (Squire LR, ed), pp 121–130. Oxford: Academic.

Navarrete-Opazo A, Vinit S, Dougherty BJ, Mitchell GS (2015) Daily acute intermittent hypoxia elicits functional recovery of diaphragm and inspiratory intercostal muscle activity after acute cervical spinal injury. Exp Neurol 266:1–10. CrossRef Medline

Navarrete-Opazo A, Dougherty BJ, Mitchell GS (2017a) Enhanced recovery of breathing capacity from combined adenosine 2A receptor inhibition and daily acute intermittent hypoxia after chronic cervical spinal injury. Exp Neurol 287:93–101. CrossRef Medline

Navarrete-Opazo A, Alcayaga J, Sepúlveda O, Rojas E, Astudillo C (2017b) Repetitive intermittent hypoxia and locomotor training enhances walking function in incomplete spinal cord injury subjects: A randomized, triple-blind, placebo-controlled clinical trial. J Neurotrauma 34:1803–1812. CrossRef Medline

Nichols NL, Mitchell GS (2016) Quantitative assessment of integrated phrenic nerve activity. Respir Physiol Neurobiol 226:81–86. CrossRef Medline

Nichols NL, Dale EA, Mitchell GS (2012) Severe acute intermittent hypoxia elicits phrenic long-term facilitation by a novel adenosine-dependent mechanism. J Appl Physiol 112:1678–1688. CrossRef Medline

Nichols NL, Gowing G, Satriotomo I, Nashold LJ, Dale EA, Suzuki M, Avalos P, Mulcrone PL, McHugh J, Svendsen CN, Mitchell GS (2013) Intermittent hypoxia and stem cell implants preserve breathing capacity in a rodent model of amyotrophic lateral sclerosis. Am J Respir Crit Care Med 187:535–542. CrossRef Medline

Nichols NL, Satriotomo I, Harrigan DJ, Mitchell GS (2015) Acute intermittent hypoxia induced phrenic long-term facilitation despite increased SOD1 expression in a rat model of ALS. Exp Neurol 273:138–150. CrossRef Medline

Peng YJ, Prabhakar NR (2004) Effect of two paradigms of chronic intermittent hypoxia on carotid body sensory activity. J Appl Physiol 96:1236–1242; discussion 1196. Medline

Prosser-Loose EJ, Hassan A, Mitchell GS, Muir GD (2015) Delayed intervention with intermittent hypoxia and task training improves forelimb function in a rat model of cervical spinal injury. J Neurotrauma 32:1403–1412. CrossRef Medline

Rosen DR, Siddique T, Patterson D, Figlewicz DA, Sapp P, Hentati A, Donaldson D, Goto J, O'Regan JP, Deng HX (1993) Mutations in Cu/Zn superoxide dismutase gene are associated with familial amyotrophic lateral sclerosis. Nature 362:59–62. CrossRef Medline

Satriotomo I, Nashold LJ, Svendsen CN, Mitchell GS (2006) Enhancement of BDNF and serotonin terminal density in phrenic and hypoglossal motor nuclei in a rat model of amyotrophic lateral sclerosis (ALS) [abstract]. FASEB J 20:A1212.

Satriotomo I, Dale EA, Dahlberg JM, Mitchell GS (2012) Repetitive acute intermittent hypoxia increases expression of proteins associated with plasticity in the phrenic motor nucleus. Exp Neurol 237:103–115. CrossRef Medline

Singh D, Verma R, Garg RK, Singh MK, Shukla R, Verma SK (2011) Assessment of respiratory functions by spirometry and phrenic nerve studies in patients of amyotrophic lateral sclerosis. J Neurol Sci 306:76–81. CrossRef Medline

Suzuki M, McHugh J, Tork C, Shelley B, Klein SM, Aebischer P, Svendsen CN (2007) GDNF secreting human neural progenitor cells protect dying motor neurons, but not their projection to muscle, in a rat model of familial ALS. PLoS One 2:e689. CrossRef Medline

Tester NJ, Fuller DD, Fromm JS, Spiess MR, Behrman AL, Mateika JH (2014) Long-term facilitation of ventilation in humans with chronic spinal cord injury. Am J Respir Crit Care Med 189:57–65. CrossRef Medline

Trumbower RD, Jayaraman A, Mitchell GS, Rymer WZ (2012) Exposure to acute intermittent hypoxia augments somatic motor function in humans with incomplete spinal cord injury. Neurorehabil Neural Repair 26:163–172. CrossRef Medline

Walker JKL, Jennings DB (1995) Metabolic change induced by phenylephrine infusion stimulates ventilation, despite increased blood pressure, in conscious rats [abstract]. FASEB J 9:A565.

Watson C, Paxinos G, Kayalioglu G (2009) The spinal cord: a Christopher and Dana Reeve Foundation text and atlas. London: Academic.

Wilkerson JE, Mitchell GS (2009) Daily intermittent hypoxia augments spinal BDNF levels, ERK phosphorylation and respiratory long-term facilitation. Exp Neurol 217:116–123. CrossRef Medline

Zinman L, Cudkowicz M (2011) Emerging targets and treatments in amyotrophic lateral sclerosis. Lancet Neurol 10:481–490. CrossRef Medline